NME7 is a functional component of the γ-tubulin ring complex

Pengfei Liu[a,b,*], Yuk-Kwan Choi[a,*], and Robert Z. Qi[a,b]
[a]Division of Life Science and State Key Laboratory of Molecular Neuroscience and [b]Nanoscience and Nanotechnology Program, Hong Kong University of Science and Technology, Kowloon, Hong Kong, China

ABSTRACT As the primary microtubule nucleator in animal cells, the γ-tubulin ring complex (γTuRC) plays a crucial role in microtubule organization, but little is known about how the activity of the γTuRC is regulated. Recently, isolated γTuRC was found to contain NME7, a poorly characterized member of the NME family. Here we report that NME7 is a γTuRC component that regulates the microtubule-nucleating activity of the γTuRC. NME7 contains two putative kinase domains, A and B, and shows autophosphorylating activity. Whereas domain A is involved in the autophosphorylation, domain B is inactive. NME7 interacts with the γTuRC through both A and B domains, with Arg-322 in domain B being crucial to the binding. In association with the γTuRC, NME7 localizes to centrosomes throughout the cell cycle and to mitotic spindles during mitosis. Suppression of NME7 expression does not affect γTuRC assembly or localization to centrosomes, but it does impair centrosome-based microtubule nucleation. Of importance, wild-type NME7 promotes γTuRC-dependent nucleation of microtubules, but kinase-deficient NME7 does so only poorly. These results suggest that NME7 functions in the γTuRC in a kinase-dependent manner to facilitate microtubule nucleation.

Monitoring Editor
Stephen Doxsey
University of Massachusetts

Received: Jun 24, 2013
Revised: Apr 23, 2014
Accepted: Apr 30, 2014

INTRODUCTION

The microtubule network is a part of the cytoskeleton that plays an essential role in a wide variety of cellular activities, including cell division, polarization, motility, and morphogenesis. The nucleation and arrayed organization of microtubules depend on the centrosome, which is known as the microtubule-organizing center. The microtubule-nucleating activity of centrosomes varies during the cell cycle, being weakest in the G1 phase and strongest during mitosis, a change that is concurrent with variations in centrosomal volume, as well as with the levels of centrosomal γ-tubulin (Doxsey *et al.*, 2005; Luders and Stearns, 2007). In interphase cells, centrosomes play a major role in microtubule nucleation, whereas during mitosis at least two additional mechanisms promote microtubule nucleation and hence spindle assembly: chromatin-based nucleation and microtubule-dependent amplification of spindle microtubules (Luders and Stearns, 2007). Both of these acentrosomal mechanisms also depend on the presence of γ-tubulin (Luders *et al.*, 2006; Goshima *et al.*, 2008; Zhu *et al.*, 2008; Mishra *et al.*, 2010). Therefore, γ-tubulin is the principal nucleator of cellular microtubules.

In animal cells, γ-tubulin is present in two complexes of distinct size: the γ-tubulin small complex (γTuSC) and the γ-tubulin ring complex (γTuRC). The γTuSC is ~300 kDa in size and comprises γ-tubulin and two other conserved proteins, GCP2 and GCP3. Multiple copies of γ-tubulin, GCP2, and GCP3 are assembled with GCP4, GCP5, and GCP6 into the macromolecular structure of the γTuRC. The *Drosophila* γTuSC exhibits minimal microtubule-nucleating activity, whereas the γTuRC nucleates microtubules substantially more efficiently (~150-fold faster; Oegema *et al.*, 1999). These observations suggest that the γTuRC but not the γTuSC is a major nucleator of microtubules. Electron microscopy reveals that the γTuRC forms a minus-end cap of microtubules (Keating and Borisy, 2000; Moritz *et al.*, 2000; Wiese and Zheng, 2000) and that the budding yeast γTuSC assembles into a γTuRC-like ring structure with a 13-fold symmetry identical to cellular microtubules (Kollman *et al.*, 2010). These studies provide compelling evidence that the γTuRC serves as a template for microtubule nucleation.

This article was published online ahead of print in MBoC in Press (http://www.molbiolcell.org/cgi/doi/10.1091/mbc.E13-06-0339) on May 7, 2014.

*These authors contributed equally to this work.

Address correspondence to: Robert Z. Qi (qirz@ust.hk).

Abbreviations used: γTuRC, γ-tubulin ring complex; γTuSC, γ-tubulin small complex.

Several additional components of the γTuRC have recently been identified, including Mozart1, GCP8 (also known as FAM128A/B and Mozart2), and NME7 (also known as NM23-H7 and NDPK7; Choi *et al.*, 2010; Hutchins *et al.*, 2010; Teixido-Travesa *et al.*, 2010). NME7 is a putative member of the NME family of multifunctional enzymes that appear to act as nucleoside-diphosphate kinases and protein histidine kinases (Lacombe *et al.*, 2000; Postel, 2003; Besant and Attwood, 2005; Bilitou *et al.*, 2009). The NME7 transcript is detected in several tissues (Lacombe *et al.*, 2000), suggesting wide expression of the protein. In this study, we investigated the interaction of NME7 with the γTuRC and the involvement of NME7 in γTuRC-mediated microtubule nucleation. We show that NME7 and its kinase activity are required for efficient microtubule nucleation.

RESULTS

Characterization of NME7

Two alternatively spliced sequences of NME7 were found in GenBank databases. These sequences are identical except for a 36–amino acid fragment that is lacking at the amino terminus of isoform B (Figure 1A). Sequence analysis predicted that NME7 contains a DM10 domain followed by two kinase domains, domains A and B. To characterize NME7, we raised antibodies that recognize both NME7 isoforms. Immunoblotting showed that the purified antibodies stained a single protein band of ~43 kDa in extracts of asynchronous HEK293T (Figure 1B; untransfected). We designed two *nme7*-targeting small interfering RNA (siRNA) oligonucleotides, and the transfection of either siRNA eliminated ~83% of the NME7 protein in HEK293T cells (Figure 1C). These results demonstrated the specificity of our anti-NME7 antibodies. We also transiently expressed the two NME7 isoforms (NME7a and NME7b) found in GenBank; on immunoblots, endogenous NME7 was identical in size to the transfected NME7a but was larger than NME7b (Figure 1B). Therefore, we conclude that NME7a is the single NME7 species detected in asynchronous cells. Similar results were obtained from several other cell lines tested, including HeLa, RPE-1, and U2OS. In mitotically arrested HeLa cells, NME7 was expressed at similar levels as in asynchronous cells.

NME7 contains two putative kinase domains and thus is a unique member of the NME family (Lacombe *et al.*, 2000). Here we tested NME7 for kinase activities. In NME1 and NME2 (also known as NM23-H1 and NM23-H2, respectively), the nucleoside-diphosphate kinase action involves the formation of an enzyme intermediate that is autophosphorylated at His-118, a highly conserved histidine in NME family members; replacement of His-118 with Phe eliminates the kinase activities of NME proteins (Postel and Ferrone, 1994; Webb *et al.*, 1995; Freije *et al.*, 1997; Gonin *et al.*, 1999). We generated NME7 mutants in which His-206 and His-355 were singly mutated to Phe; His-206 and His-355 in kinase domains A and B, respectively, are the residues corresponding to His-118 (Figure 2A). To test for autophosphorylation, we expressed the wild-type and mutant proteins in and purified from bacteria. In autophosphorylation assays, both the wild-type protein and the H355F mutant were readily phosphorylated in reactions containing either ATP or GTP as the γ-phosphate donor, whereas the H206F mutant was not autophosphorylated at detectable levels (Figure 2, B and C). Mutational analyses of NME1/2 identified other residues crucial for kinase activity, including Arg-88 (Lacombe *et al.*, 2000). In NME7, Lys-173 and Arg-322 of kinase domains A and B, respectively, are the residues corresponding to Arg-88 (Figure 2A). We therefore generated another set of kinase-domain mutants by substituting Lys-173 and Arg-322 with Ala. Autophosphorylation was abolished by the K173A mutation but was unaffected by the R322A mutation (Figure 2B). Thus,

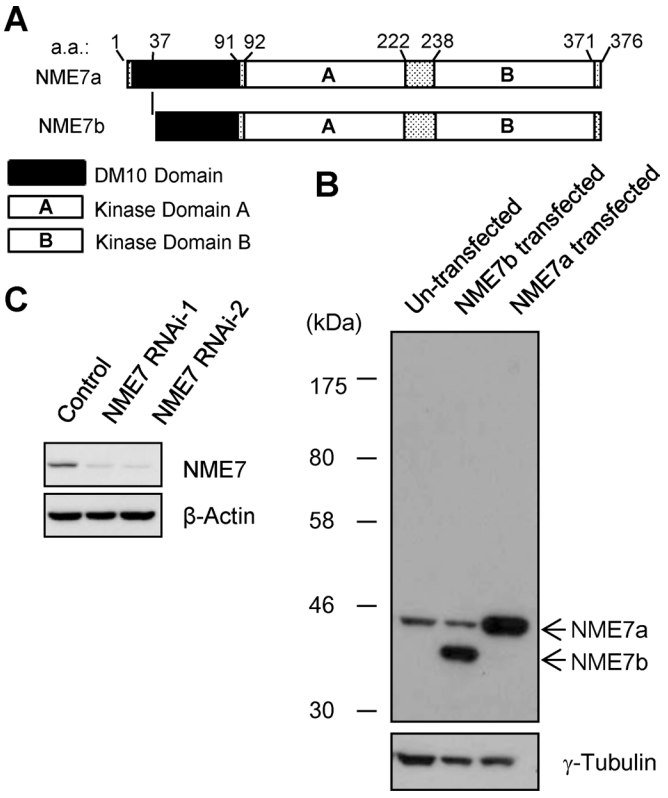

FIGURE 1: NME7 is detected in cultured cells and depleted after RNAi. (A) Schematic representation of NME7 domains. (B) Detection of NME7 isoforms. Lysates of HEK293T cells were probed using anti-NME7 and anti–γ-tubulin antibodies. Cells transfected with NME7a or NME7b were also analyzed by means of anti-NME7 immunoblotting. (C) HEK293T cells transfected with siRNA oligonucleotides were immunoblotted with anti-NME7 and anti–β-actin antibodies. The intensity of NME7 bands was quantified and normalized relative to the corresponding β-actin bands to estimate RNAi efficiency.

two separate mutations in domain A eliminated NME7 autophosphorylation, whereas the corresponding mutations in domain B were ineffective in doing so. These results indicate that domain A but not domain B possesses kinase activity.

As nucleoside-diphosphate kinases, several NME members catalyze the production of nucleoside triphosphates by transferring the γ-phosphate from a nucleoside triphosphate to a nucleoside diphosphate (Lacombe *et al.*, 2000; Postel, 2003; Bilitou *et al.*, 2009). However, we did not observe any nucleoside-diphosphate kinase activity in NME7 by using in vitro assays in which we measured the transfer of γ-phosphate from either ATP or GTP (unpublished data). These results agree with the findings of others (Yoon *et al.*, 2005).

The subcellular localization of NME7 was examined in proliferating cells at different cell cycle stages. In interphase cells, NME7 was stained at the centrosomes, which were labeled with an anti–γ-tubulin antibody (Figure 3A). Furthermore, NME7 showed nuclear localization and general low-level distribution in the cytoplasm (Figure 3A). After centrosomal duplication, NME7 was localized equally at both centrosomes in cells (Figure 3A), and, during mitosis, staining for NME7 was detected at mitotic spindles in addition to centrosomes, displaying a similar pattern as γ-tubulin (Figure 3A). The centrosomal content of NME7 changed during the cell cycle: the level was lowest in early G1 phase and highest in metaphase, which correlated closely with the changes in γ-tubulin levels

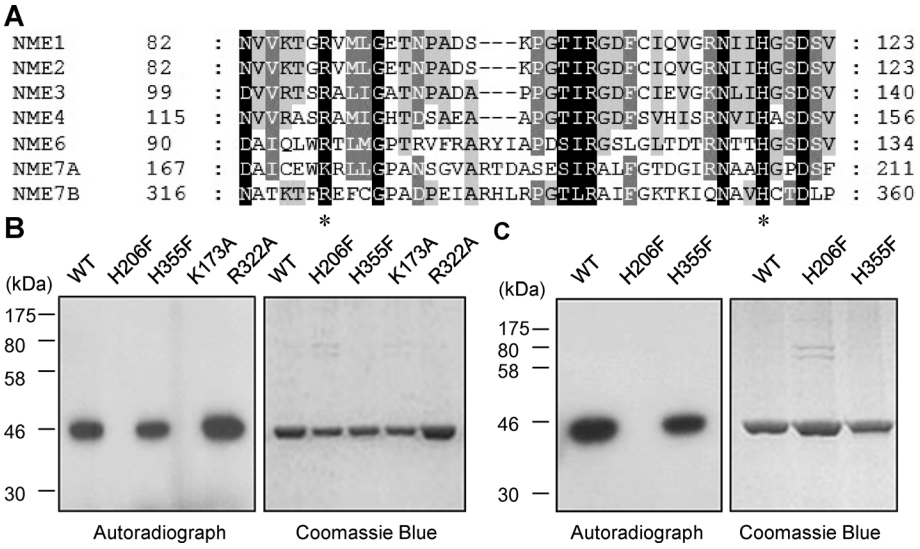

FIGURE 2: NME7 undergoes autophosphorylation. (A) Sequence alignment of the putative kinase domains (NME7A and NME7B) of NME7 with those of other members of the NME family. Asterisks indicate the residues targeted using site-directed mutagenesis. (B, C) Recombinant NME7 (WT) and its mutants were subjected to an autophosphorylation reaction in which either [γ-^{32}P]ATP (B) or [γ-^{32}P]GTP (C) was used as the phosphate donor. After the reaction, proteins were resolved using SDS–PAGE and examined by means of Coomassie blue staining and autoradiography. H206F, H355F, K173A, and R322A are the mutants.

(Figure 3A). NME7 also appeared on the central spindle in late anaphase and in the midbody during cytokinesis (Figure 3A). These localization patterns are specific, because anti-NME7 antibodies showed only background staining in cells in which NME7 was depleted through RNA interference (RNAi; Figure 3A).

To further confirm the centrosomal localization of NME7, we isolated centrosomes biochemically from HEK293T cells. NME7 was specifically coisolated with centrosomes, which were probed by immunoblotting for the centrosomal proteins γ-tubulin, GCP5, and CDK5RAP2 (Figure 3B). Therefore, our immunostaining and biochemical purification assays both demonstrated that NME7 is a centrosomal protein. NME7 localization at centrosomes was largely independent of microtubules, because NME7 remained on the centrosomes after exposure to cold temperatures (see later discussion of Figure 6) or nocodazole (unpublished data).

Association of NME7 with the γTuRC

To investigate the association of NME7 with the γTuRC, we first immunoprecipitated NME7; in these anti-NME7 immunoprecipitates, γ-tubulin and GCP2-6 were readily detected (Figure 4A). In a reciprocal experiment, NME7 was found in anti-GCP5 immunoprecipitates, which also contained other γTuRC components (Figure 4A). Next we analyzed the distribution of NME7 and γTuRC components by sedimenting cell extracts through a sucrose gradient. A part of cellular NME7 cosedimented with the γTuRC, but most of the NME7 was detected in fractions containing small-molecular species (Figure 4B). The fractions of the sucrose gradient were next used in immunoprecipitation assays. NME7 coimmunoprecipitated with γ-tubulin and GCPs from the pooled γTuRC fractions but failed to coprecipitate with these proteins from the low–molecular weight fractions containing γ-tubulin (Figure 4C), which demonstrated that NME7 associates with the γTuRC but not with γ-tubulin present as smaller-molecular species. Moreover, NME7 immunodepletion experiments showed that only a small subset of cytosolic γTuRC contains NME7, and, in accord with these results, inhibition of NME7 expression did not alter the fractionation patterns of the γTuRC proteins (Figure 4D). These results indicate that NME7 is dispensable for γTuRC assembly.

To map the γTuRC-binding domain in NME7, we ectopically expressed fragments of NME7 in cells for use in immunoprecipitation experiments. Both A and B kinase domains were required for coimmunoprecipitating γ-tubulin, whereas the DM10 domain was dispensable (Figure 4E). Therefore, the γTuRC binds to a structural motif assembled using both kinase domains of NME7. Through mutational analysis, we next identified Arg-322, a conserved residue in kinase domain B, as being crucially involved in γTuRC binding: changing Arg-322 to Ala substantially reduced the coimmunoprecipitation of NME7 and proteins of the γTuRC; changing Arg-322 to Glu abolished the coimmunoprecipitation (Figure 4F).

To probe whether NME7 and the γTuRC require each other for centrosomal localization, we silenced the cellular expression of NME7, γ-tubulin, and GCP4 individually. Our RNAi-mediated knockdowns were effective and specific, reducing the expression of targeted proteins but not unrelated proteins (Figure 5A). The depletion of NME7 had little effect on the centrosomal staining of γ-tubulin and GCP4 (Figure 5B), indicating that NME7 is not required for the centrosomal localization of the γTuRC. Moreover, the centrosomal localization of CDK5RAP2, a pericentriolar material protein associated with the γTuRC (Fong *et al.*, 2008; Choi *et al.*, 2010), was not altered noticeably after NME7 depletion (unpublished data). When siRNAs targeting γ-tubulin or GCP4 were transfected into cells, NME7 staining at centrosomes decreased substantially, which correlated closely with the reduced centrosomal levels of γ-tubulin (Figure 5, B and C). Thus, we conclude that the centrosomal localization of NME7 depends on the assembly of NME7 into the γTuRC. Suppression of GCP4 expression is known to disrupt γTuRC assembly (Verollet *et al.*, 2006; Choi *et al.*, 2010). Here depletion of GCP4 potently inhibited the centrosomal localization of γ-tubulin (Figure 5, B and C), indicating that the formation of the γTuRC is a prerequisite for γ-tubulin attachment to centrosomes.

NME7 in γTuRC-mediated microtubule nucleation

To determine whether NME7 is involved in microtubule nucleation at centrosomes, we compared microtubule regrowth in control cells and in cells in which NME7 was depleted through RNAi. In this assay, microtubule regrowth was initiated after cold-induced depolymerization by shifting cells to 37°C. At 1.5 min of regrowth, prominent asters of microtubules formed in control cells, but markedly smaller asters were found in the NME7-depleted cells (Figure 6A). At 2.5 min of regrowth, control cells displayed long microtubules emanating from the centrosomal aster, whereas NME7-depleted cells showed asters with sparser microtubules (Figure 6A). However, after ≥5 min, both control and NME7-depleted cells had established extensive microtubule arrays that were centered at the centrosomes (Figure 6A). As a complementary approach, we performed live-cell imaging of an EB1–green fluorescent protein (GFP) stable cell line to assess the microtubule-nucleating ability of centrosomes. In this stable line, EB1-GFP is expressed at a low level and thus labels the

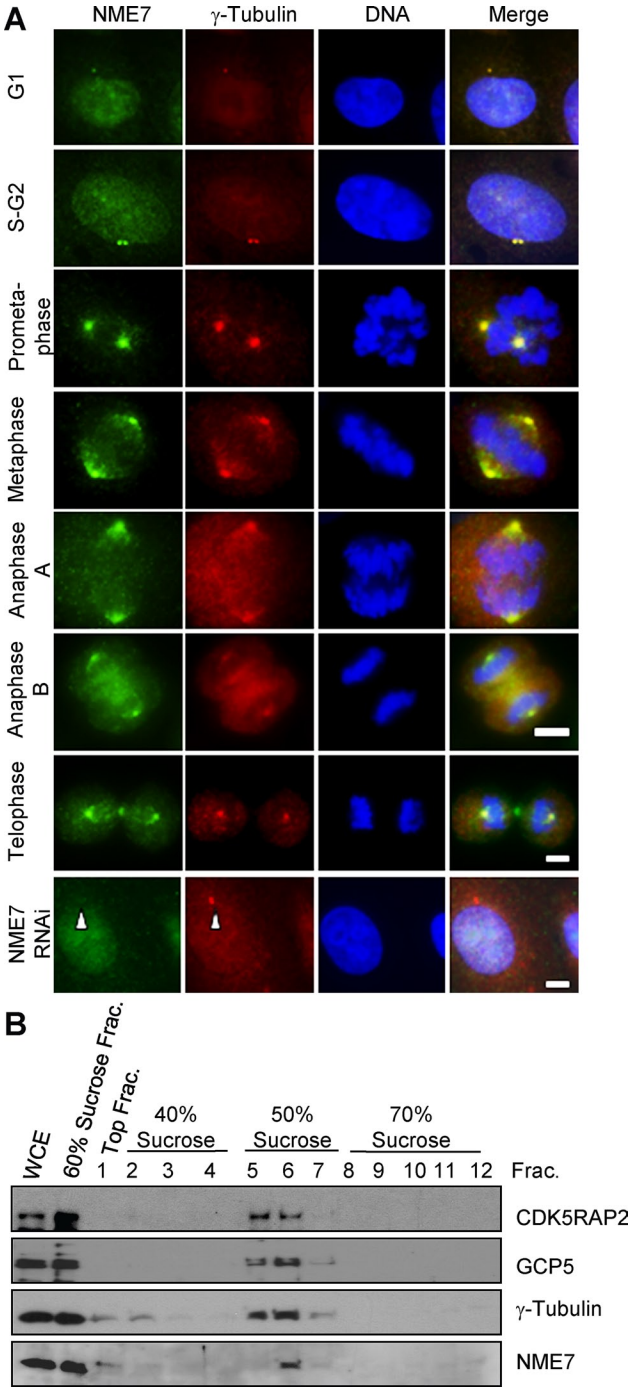

FIGURE 3: NME7 is a centrosomal protein. (A) Immunofluorescence micrographs of hTERT-RPE1 cells stained for NME7 and γ-tubulin; DNA was visualized using Hoechst33258. Arrows indicate centrosomes. Scale bars, 5 μm. (B) Cosedimentation of NME7 with centrosomes. Centrosomes were isolated by sequential centrifugation over 60% sucrose and then over a discontinuous sucrose gradient. All gradient fractions were immunoblotted for NME7 and centrosomal proteins as indicated. WCE, whole-cell extract.

plus end of growing microtubules (Fong *et al.*, 2009). To minimize cell cycle–related variations (Piehl *et al.*, 2004), microtubule nucleation was measured in cells of similar cell cycle stages (i.e., of G_1/S cells). The depletion of NME7 reduced the number of EB1-GFP comets emanating from the centrosomes by ~48% (control RNAi: 18.6 ± 2.9 microtubules/min; NME7 RNAi: 9.8 ± 3.4 microtubules/min; Figure 6B). Thus, the results of both assays demonstrated that microtubule nucleation by centrosomes was markedly diminished in cells depleted of NME7.

We next examined the potential effect of NME7 on γTuRC-mediated microtubule nucleation by using an assay described previously (Choi *et al.*, 2010). The γTuRC was isolated using the γTuRC-binding domain of CDK5RAP2 (Choi *et al.*, 2010), and wild-type and mutant NME7 proteins were expressed in and purified from bacteria. In the absence of the γTuRC, NME7 displayed negligible microtubule-nucleation activity, and the γTuRC by itself nucleated microtubules only weakly (Figure 7). Adding NME7 increased the microtubule-nucleating activity of the γTuRC in a dose-dependent manner, to a maximum of ~2.5-fold with the addition of 222 nM NME7 (Figure 7, A and B). By contrast, the activity was not affected significantly after adding this amount of the NME7 R322A mutant, which does not bind the γTuRC (Figure 7A). Therefore, the association with NME7 enhances the microtubule-nucleation activity of the γTuRC. To explore whether the kinase activity of NME7 is required for promoting nucleation, we tested the kinase-deficient mutant K173A: the mutant protein promoted γTuRC-dependent microtubule nucleation by ~58%, which was considerably weaker than the activation by wild-type NME7 (Figure 7). Thus, NME7 promoted, in a kinase activity-dependent manner, the microtubule-nucleating activity of the γTuRC.

DISCUSSION

The molecular regulation and assembly of the γTuRC—the principal microtubule nucleator in cells—are incompletely understood. We and others identified the NME7 protein in isolated γTuRC (Choi *et al.*, 2010; Hutchins *et al.*, 2010; Teixido-Travesa *et al.*, 2010). In this study, we characterized NME7 and demonstrated the involvement of NME7 in γTuRC-initiated nucleation of microtubules.

We determined that NME7 is a centrosomal protein that is localized at centrosomes through its assembly into the γTuRC. The centrosomal content of NME7 varies during the cell cycle, being highest in mitosis and lowest in early G1; this correlates closely with the changes in γ-tubulin levels. The use of high-resolution microscopy reveals that the pericentriolar material is organized in concentric toroids around the mother centriole, with various proteins forming distinct layers (Lawo *et al.*, 2012; Mennella *et al.*, 2012; Sonnen *et al.*, 2012). For example, Cep120 is present at the inner layer close to the centriole, whereas microtubule-nucleating factors such as the γTuRC and CDK5RAP2 are located in layers farther from the centriole; these outer layers may contain NME7 together with the γTuRC. Because NME7 was found to be dispensable for the centrosomal localization of γ-tubulin and CDK5RAP2, NME7 might not serve as a structural component of the pericentriolar material but might function as a regulator of γTuRC in centrosomes.

In mammals, the NME family contains at least 10 members (Boissan *et al.*, 2009; Desvignes *et al.*, 2009); all NME proteins possess a single kinase domain, except for the NME7 and NME8 proteins, which have two and three putative kinase domains, respectively. Both kinase domains of NME7 display high homologies to the kinase domains found in other NMEs, although with substitutions of certain residues involved in kinase activity (Figure 2A; Lacombe *et al.*, 2000). Our autophosphorylation-assay results demonstrated unequivocally that NME7 is an active kinase that catalyzes phosphate transfer from ATP or GTP. Furthermore, kinase domain A is catalytically active, but domain B is a pseudokinase domain. Of interest, domain B is critical for interaction with the γTuRC, because the substitution of Arg-322 in domain B reduced dramatically or even eliminated NME7–γTuRC binding. NME7 does not contain the GRIP motifs found in GCP2-6

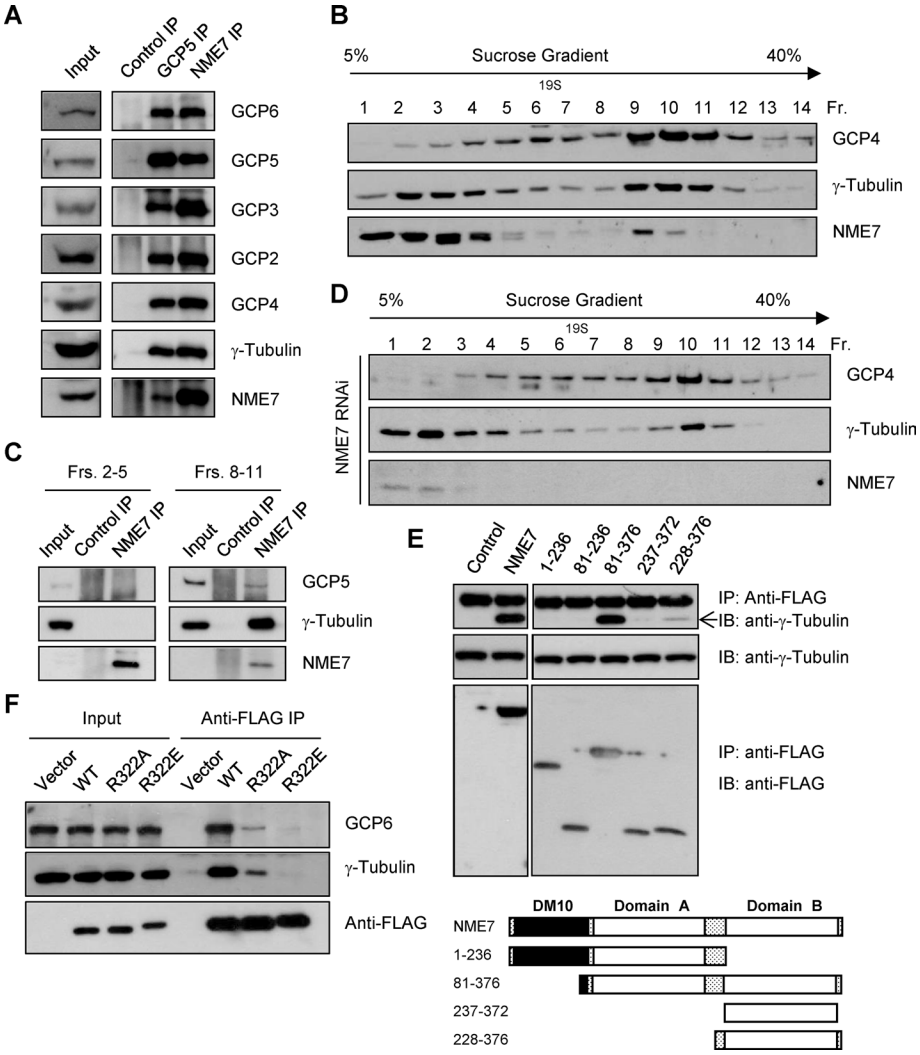

FIGURE 4: NME7 is a component of the γTuRC. (A) Proteins were immunoprecipitated from HEK293T extracts by using anti-NME7, anti-GCP5, and anti–immunoglobulin G (control) antibodies, and the immunoprecipitates were probed by means of immunoblotting. (B) HEK293T extracts were fractionated by centrifuging them over a continuous sucrose gradient, and the gradient fractions obtained were immunoblotted. (C) Gradient fractions containing γ-tubulin of the low–molecular weight species (fractions 2–5) and the γTuRC (fractions 8–11) were pooled and used for anti-NME7 immunoprecipitation. The immunoprecipitates were probed by means of immunoblotting. (D) Sucrose-gradient fractions of extracts of HEK293T cells transfected with an *nme7*-targeting siRNA (NME7 RNAi) were probed on immunoblots. (E) Extracts of HEK293T cells expressing FLAG-tagged NME7 fragments were used for immunoprecipitation with an anti-FLAG antibody. The precipitated proteins were immunoblotted for γ-tubulin and NME7 fragments (anti-FLAG). A schematic representation of the NME7 constructs is shown below. (F) Extracts of HEK293T cells expressing FLAG-tagged wild-type (WT) and mutant NME7 proteins were immunoprecipitated with anti-FLAG antibodies. The precipitates were probed using anti–γ-tubulin, anti-FLAG, and anti-GCP6 antibodies.

(Wiese and Zheng, 2006), but instead uses a large region encompassing domains A and B for assembly into the γTuRC. Consistent with this requirement of both kinase domains for γTuRC binding, NME1, 5, 6, and 10, which contain a single kinase domain, fail to interact with the γTuRC (unpublished data). Whether NME8 binds the γTuRC remains unknown, raising the possibility that NME7 is a unique member of the NME family that functions in the γTuRC.

NME7 promoted γTuRC-induced microtubule nucleation in the reconstitution assay used in this study. The extent of activation observed after adding exogenous NME7 is likely underestimated because the isolated γTuRC contained a small amount of endogenous NME7; we have been unable to purify large amounts of NME7-free γTuRC. We also found that the kinase function of NME7 is involved in promoting nucleation, but the targets of NME7 in the γTuRC are unknown. NME7 could act in the following ways. First, NME7 might promote the conversion of γ-tubulin from a GDP- to a GTP-bound form within the γTuRC, although the nucleoside-diphosphate kinase activity of NME7 has not been observed (Yoon *et al.*, 2005; this study). Structural studies show that γ-tubulin adopts a curved conformation that is similar to that of GDP-bound α/β-tubulin and thus is apparently unfavorable for nucleation reactions (Aldaz *et al.*, 2005; Rice *et al.*, 2008). Furthermore, γ-tubulin does not undergo any conformational change upon shifting from the GDP- to the GTP-bound state. Therefore, the function of the shift from GDP to GTP on γ-tubulin is unclear, but γ-tubulin appears to require its binding to GDP/GTP for microtubule organization: mutations of the nucleotide-binding domain of γ-tubulin are deleterious (Hendrickson *et al.*, 2001; Jung *et al.*, 2001; Gombos *et al.*, 2013). Second, NME7 might catalyze protein phosphorylation in the γTuRC. Because the original NME family members NME1/2 are protein histidine kinases (Besant and Attwood, 2005; Kee and Muir, 2012), an interesting question is whether NME7 also phosphorylates histidine residues in its substrates. Several γTuRC components, including γ-tubulin, GCP5, and GCP6, are phosphorylated at Ser/Thr and/or Tyr (Vogel *et al.*, 2001; Izumi *et al.*, 2008; Alvarado-Kristensson *et al.*, 2009; Lin *et al.*, 2011; Bahtz *et al.*, 2012), but whether γ-tubulin and GCPs undergo histidine phosphorylation is unknown. Overall our data reveal that NME7 is a modulator of the γTuRC activity, which is consistent with the observation that NME7 is not required for γTuRC assembly but is still present in a fraction of the cellular γTuRC.

At centrosomes, γ-tubulin participates in centriole duplication and primary cilium assembly, in addition to performing microtubule-nucleating and -organizing functions (Haren *et al.*, 2006; Mikule *et al.*, 2007). RNAi-mediated depletion of NME7 did not affect centriole duplication and cell mitosis noticeably, but NME7-depleted cells grew slightly more slowly than normal cells (unpublished results). This is reminiscent of the observations made after depleting GCP8/Mozart2/FAM128, a γTuRC component that might help organize interphase microtubules (Teixido-Travesa *et al.*, 2010). Mice with homozygous deletion of *nme7* developed situs inversus, hydrocephalus, and a thinning of the cerebral cortex, implicating a role of NME7 in cilium formation and function (Vogel *et al.*, 2010). In an RNAi functional screen, NME7 was identified as a protein required

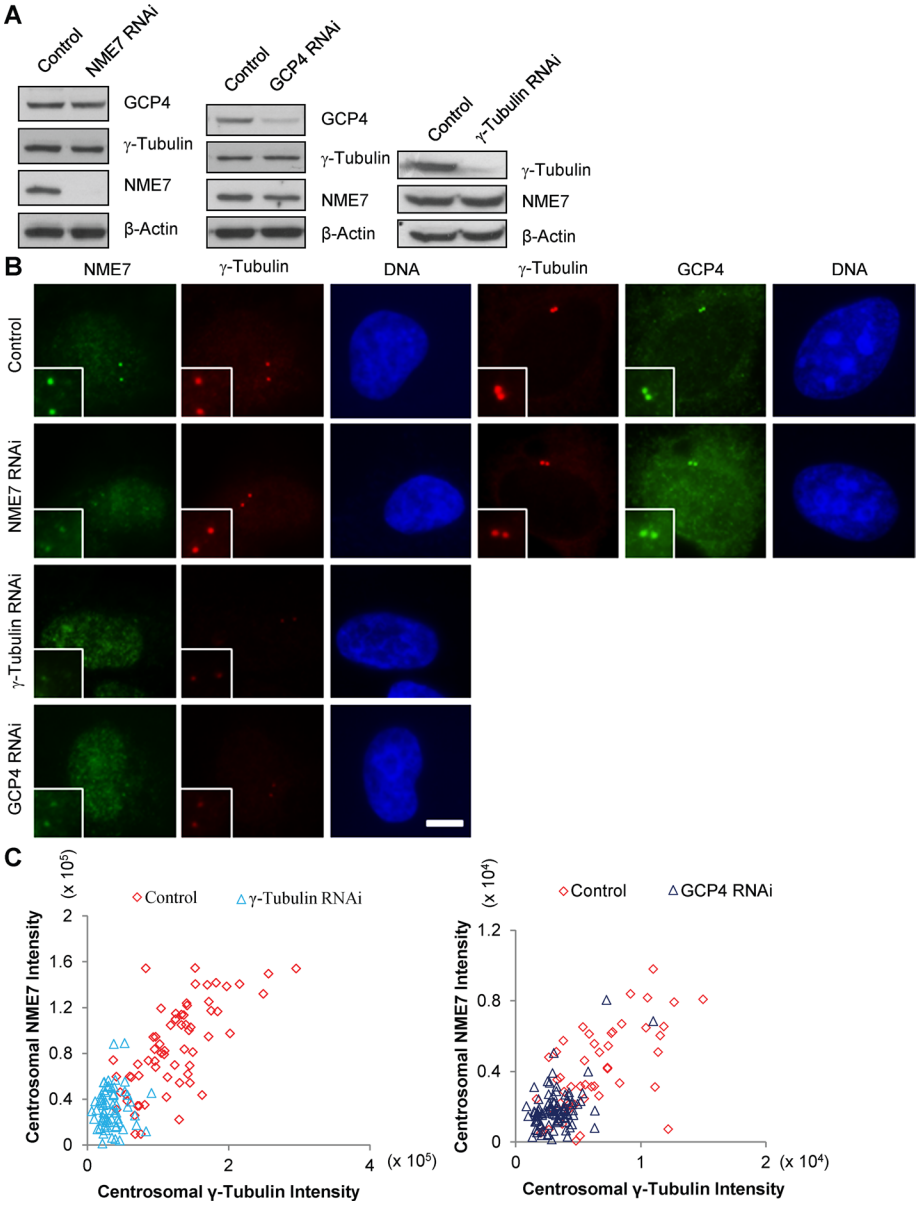

FIGURE 5: NME7 localizes at centrosomes through assembly into the γTuRC. (A) HeLa cells were transfected with a control siRNA or with siRNAs against NME7, γ-tubulin, or GCP4. Protein expression was analyzed by means of immunoblotting. (B) siRNA-transfected cells were immunostained and examined using fluorescence microscopy. Boxed areas show magnified centrosomes. Scale bar, 5 μm. (C) Centrosomal intensities of NME7 and γ-tubulin were measured in cells transfected with siRNAs targeting γ-tubulin or GCP4. Data are presented after background subtraction; the data shown are representative of three independent experiments.

for ciliary signaling and protein trafficking to primary cilia, and NME7 was detected on the basal body but not in the cilia (Lai *et al.*, 2011). By elucidating the function of NME7 in the γTuRC, this study enhances our understanding of how NME7 contributes to basal-body organization and to the control of ciliary transport.

MATERIALS AND METHODS

Plasmids and siRNA oligonucleotides

The entire coding sequence of human NME7 (GenBank accession NM_013330.3) was obtained from OriGene (Rockville, MD) and cloned into expression vectors by using standard cloning techniques. Site-directed mutagenesis was performed using PCR-based methods. Two siRNA oligonucleotide duplexes targeting NME7 were synthesized: 5′-GUGAAGGACUGUUGGGAAA-3′ (siNME7-1) and 5′-GGGUUAAUGUUGAGGAAUU-3′ (siNME7-2). The siRNA oligonucleotides targeting GCP4 (5′-GCAAUCAAGUGGCGCCUAA-3′) and γ-tubulin (5′-AGGAGGACAUGUUCAAGGA-3′) were used as previously described (Choi *et al.*, 2010).

Recombinant proteins and antibodies

Recombinant proteins containing a hexahistidine (His_6) or glutathione *S*-transferase (GST) tag were expressed in *Escherichia coli* BL21 (DE3) and then isolated using Ni^{2+}-nitrilotriacetic acid resin (Qiagen, Valencia, CA) or GSH-Sepharose (GE Healthcare, Chalfont St. Giles, Buckinghamshire, United Kingdom), respectively. After elution, the proteins were dialyzed in 50 mM Tris-HCl, pH 7.4, 150 mM NaCl, 1 mM ethylene glycol tetraacetic acid (EGTA), and 10% glycerol and then stored at –80°C.

Two anti-NME7 antisera were generated by immunizing rabbits with NME7 1–140 and full-length NME7 prepared as His_6-tagged proteins. The sera obtained were named sera 651 and 673, respectively. Both antibodies were purified using respective antigens in fusion with GST and immobilized on polyvinylidene fluoride membranes. The two antibodies gave similar results in experiments, and most of the data presented here were collected using antibody 651. The production of the following antibodies has been described previously: rabbit anti-CDK5RAP2, anti-GCP2, anti-GCP3, anti-GCP4, anti-GCP5, and anti-GCP6 (Fong *et al.*, 2008; Choi *et al.*, 2010). These mouse monoclonal antibodies were purchased from Sigma (St. Louis, MO): anti-FLAG (M2), anti–γ-tubulin (GTU-88), anti–α-tubulin (DM1A), and anti–β-actin (AC-15).

Cell culture and immunofluorescence microscopy

HEK293A, HEK293T, U2OS, and HeLa cells were maintained in DMEM containing 10% fetal bovine serum; hTERT-RPE1 cells were grown in DMEM/Ham's F12 (1:1) containing 10% fetal bovine serum and 10 μg/ml hygromycin B. To suppress protein expression, siRNA oligonucleotides were transfected into cells by using Lipofectamine 2000 (Invitrogen, Carlsbad, CA); targeted proteins were depleted effectively at 48–72 h after transfection.

To immunolabel NME7, cells grown on coverslips were fixed (15 min, room temperature) in 4% paraformaldehyde in PHEM buffer (60 mM 1,4-piperazinediethanesulfonic acid [PIPES], 25 mM 4-(2-hydroxyethyl)-1-piperazineethanesulfonic acid [HEPES], pH 6.9, 10 mM EGTA, and 2 mM $MgCl_2$) containing 0.5% Triton X-100. In some cases, cells were fixed in methanol at –20°C for 10 min. Fluorescence images were acquired using an inverted microscope (Eclipse TE2000; Nikon, Tokyo, Japan)

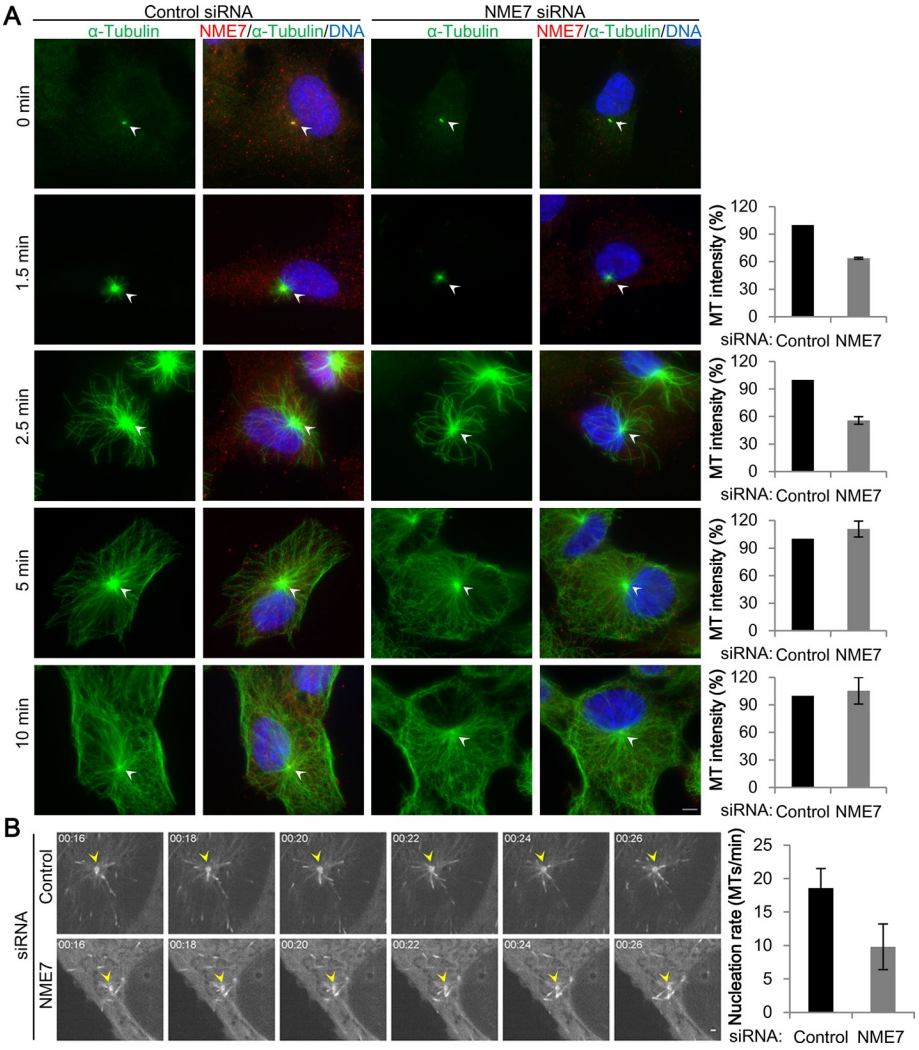

FIGURE 6: NME7 depletion impairs centrosomal microtubule nucleation. (A) The microtubule-regrowth assay was performed using hTERT-RPE1 cells transfected with control or *nme7*-targeting siRNAs. In the micrographs, arrows indicate centrosomes. Microtubule asters were quantified based on examining ~50 cells/sample in each experiment. The data are presented as relative intensities (mean ± SD) measured in three independent experiments. MT, microtubule. Scale bar, 5 μm. (B) U2OS cells stably expressing EB1-GFP were transfected with control or *nme7*-targeting siRNAs. Representative time-lapse images collected from G_1/S cells. Microtubule nucleation rates are presented as the average microtubule nucleation rate ± SD; $n = 14$ cells, control samples; $n = 17$ cells, *nme7*-depleted samples. Scale bar, 2 μm.

equipped with a SPOT RT1200 camera (Diagnostic Instruments, Sterling Heights, MI). The centrosomal intensities of NME7, γ-tubulin, and GCP4 were measured as integrated fluorescence intensities within a circle (2-μm diameter) that was centered on the centrosome. Background fluorescence obtained from the general cytoplasm by using the same circle was subtracted.

To perform microtubule regrowth, cellular microtubules were first depolymerized by incubation in ice water for 1 h, and microtubule growth was initiated by transferring the cells to 37°C; cells were then fixed at various time points and immunolabeled. Fluorescence images were acquired using a Zeiss Axio Observer Z1 microscope (Carl Zeiss, Jena, Germany) equipped with an ORCA-Flash 4.0 camera (Hamamatsu, Hamamatsu, Japan). The intensities of microtubule asters were quantified within manually defined areas tracing the microtubule ends. Data are presented after background subtraction.

Time-lapse microscopy

The generation and maintenance of a U2OS subline stably expressing low levels of EB1-GFP were reported previously (Fong *et al.*, 2009). Cells seeded on 35-mm glass-bottomed culture dishes were used for acquiring time-lapse image sequences on a spinning-disk microscope (Carl Zeiss Axio-Observer Z1; Yokogawa CSU-X1 spinning disk; Yokogawa, Japan) equipped with an Andor Neo sCMOS camera (Andor, Belfast, UK). Time-lapse sequences (30 frames for each cell) were acquired at 2-s intervals at an exposure time of 50–300 ms. Microtubule-nucleation rates were derived from the number of EB1 comets emerging from the centrosomes and are presented as average numbers of microtubules nucleated per minute.

Centrosome isolation

Centrosomes were isolated from cells as described (Moudjou and Bornens, 1994). Briefly, HEK293T cells were treated with 0.3 μg/ml nocodazole and 2 μg/ml cytochalasin B for 1.5 h at 37°C before harvesting. Cell extracts prepared in extraction buffer (1 mM HEPES, pH 7.2, 0.5 mM $MgCl_2$, 0.1% β-mercaptoethanol, and 0.5% Igepal CA-630) were clarified and then centrifuged over 60% sucrose in gradient buffer (10 mM PIPES, pH 7.2, 0.1% Triton X-100, and 0.1% β-mercaptoethanol) at 10,000 × *g* (TLS-55 rotor; Beckman Coulter, Brea, CA) for 30 min at 4°C. After centrifugation, 90% of the extracts were discarded, and the remaining samples were mixed and loaded onto a discontinuous sucrose gradient (40, 50, and 70% sucrose in gradient buffer) and centrifuged at 120,000 × *g* (TLS-55 rotor) for 1.5 h at 4°C. After centrifugation, the gradient was collected into 12 aliquots for analysis.

Sucrose-gradient centrifugation

Cell extracts were prepared in HEPES buffer (50 mM HEPES, pH 7.4, 150 mM NaCl, 1 mM $MgCl_2$, 1 mM EGTA, 0.5% Igepal CA-630, 1 mM dithiothreitol [DTT], and protease inhibitor cocktail) supplemented with 0.1 mM GTP and then clarified by means of centrifugation (20,000 × *g* for 15 min). The extracts (100 μl) were loaded onto detergent-free 2.2-ml, 5–40% sucrose gradients and centrifuged at ~200,000 × *g* (TLS-55 rotor) for 3 h. After centrifugation, the gradient was collected into 14 fractions. The molecular-mass marker thyroglobulin (19S) was run on a parallel gradient.

Autophosphorylation

To examine autophosphorylation, recombinant wild-type and mutant NME7 proteins (1 μg) were incubated for 10 min at room temperature in 10 μl of 50 mM Tris-HCl, pH 7.8, 5 mM $MgCl_2$, 1 mM DTT, 50 μM cold ATP, and 2.5 μCi of [γ-^{32}P]ATP (3000 Ci/mmol; PerkinElmer, Waltham, MA); to test GTP as the substrate, [γ-^{32}P]GTP

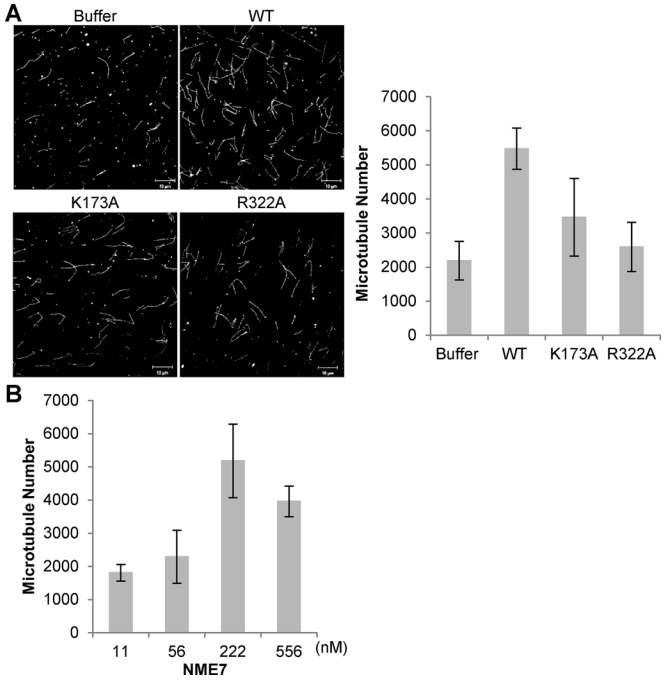

FIGURE 7: NME7 activates γTuRC-mediated microtubule nucleation in vitro. (A) Microtubules were polymerized using purified γTuRC in the absence or presence of NME7 proteins (222 nM); WT, wild-type NME7; K173A and R322A, NME7 mutants. Left, representative microscopic fields of polymerized microtubules. Scale bars, 10 μm. The bar graph presents the statistical summary of microtubule polymerization. Microtubules were counted in at least 10 random fields to calculate the average numbers of microtubules. The collected data, shown as mean ± SD of six independent experiments, were analyzed using Student's *t* test of individual pairs ($p < 0.05$ for WT vs. K173A, WT vs. R322A, WT vs. buffer, and K173A vs. buffer). (B) Microtubule-polymerization assays were performed using the γTuRC and increasing amounts of the wild-type NME7 protein; the data collected are shown as the mean ± SEM.

was used instead of ATP in the assays. Reactions were terminated by adding an equal volume of SDS–PAGE sample buffer (but without boiling). The samples were resolved by SDS–PAGE and then examined by means of autoradiography; proteins in gels were visualized using Coomassie blue staining.

Microtubule nucleation in vitro

The γTuRC was isolated from HEK293A and used to induce in vitro microtubule nucleation as described (Choi *et al.*, 2010). After FLAG-peptide elution, the eluate containing γTuRC was passed through a ZebaSpin column (Thermo Scientific, Rockford, IL) that featured a 40-kDa cut-off and was preequilibrated with buffer containing 50 mM HEPES, pH 7.2, 150 mM NaCl, 1 mM EGTA, 1 mM $MgCl_2$, 200 μM GTP, and 0.01% Igepal CA-630. Before use in microtubule-nucleation assays, NME7 was preincubated with purified γTuRC (~2 nM GCP5) at 4°C for 30 min. Microtubule-nucleation reactions were performed at 37°C for 3.5 min. After the reaction, samples were fixed in 1% glutaraldehyde and diluted, and then microtubules were sedimented onto a coverglass through a 15%-glycerol cushion in centrifuge tubes (173,000 × *g* for 8 min at 4°C; TLS-55) equipped with a Teflon platform. In each sample, the number of microtubules was determined by counting microtubules in 10 random fields under a confocal microscope (LSM Duo 710 and Zen version 1.0.0.0; Carl Zeiss).

ACKNOWLEDGMENTS

We thank Yuehong Shen and Xulun Sun for assistance in generating NME7 constructs. This work was supported by grants from the Research Grants Council (General Research Fund 662511 and 662612 and Theme-based Research Scheme) of Hong Kong, the National Key Basic Research Program of China (2013CB530900), the University Grants Committee (Area of Excellence Scheme and Special Equipment Grant) of Hong Kong, the Innovation and Technology Commission (ITCPD/17-9) of Hong Kong, the TUYF Charitable Trust, and the Nanoscience and Nanotechnology Program of the Hong Kong University of Science and Technology.

REFERENCES

Aldaz H, Rice LM, Stearns T, Agard DA (2005). Insights into microtubule nucleation from the crystal structure of human γ-tubulin. Nature 435, 523–527.

Alvarado-Kristensson M, Rodriguez MJ, Silio V, Valpuesta JM, Carrera AC (2009). SADB phosphorylation of γ-tubulin regulates centrosome duplication. Nat Cell Biol 11, 1081–1092.

Bahtz R, Seidler J, Arnold M, Haselmann-Weiss U, Antony C, Lehmann WD, Hoffmann I (2012). GCP6 is a substrate of Plk4 and required for centriole duplication. J Cell Sci 125, 486–496.

Besant PG, Attwood PV (2005). Mammalian histidine kinases. Biochim Biophys Acta 1754, 281–290.

Bilitou A, Watson J, Gartner A, Ohnuma S (2009). The NM23 family in development. Mol Cell Biochem 329, 17–33.

Boissan M, Dabernat S, Peuchant E, Schlattner U, Lascu I, Lacombe ML (2009). The mammalian Nm23/NDPK family: from metastasis control to cilia movement. Mol Cell Biochem 329, 51–62.

Choi YK, Liu P, Sze SK, Dai C, Qi RZ (2010). CDK5RAP2 stimulates microtubule nucleation by the γ-tubulin ring complex. J Cell Biol 191, 1089–1095.

Desvignes T, Pontarotti P, Fauvel C, Bobe J (2009). NME protein family evolutionary history, a vertebrate perspective. BMC Evol Biol 9, 256.

Doxsey S, McCollum D, Theurkauf W (2005). Centrosomes in cellular regulation. Annu Rev Cell Dev Biol 21, 411–434.

Fong KW, Choi YK, Rattner JB, Qi RZ (2008). CDK5RAP2 is a pericentriolar protein that functions in centrosomal attachment of the γ-tubulin ring complex. Mol Biol Cell 19, 115–125.

Fong KW, Hau SY, Kho YS, Jia Y, He L, Qi RZ (2009). Interaction of CDK5RAP2 with EB1 to track growing microtubule tips and to regulate microtubule dynamics. Mol Biol Cell 20, 3660–3670.

Freije JM, Blay P, MacDonald NJ, Manrow RE, Steeg PS (1997). Site-directed mutation of Nm23-H1. Mutations lacking motility suppressive capacity upon transfection are deficient in histidine-dependent protein phosphotransferase pathways in vitro. J Biol Chem 272, 5525–5532.

Gombos L, Neuner A, Berynskyy M, Fava LL, Wade RC, Sachse C, Schiebel E (2013). GTP regulates the microtubule nucleation activity of γ-tubulin. Nat Cell Biol 15, 1317–1327.

Gonin P, Xu Y, Milon L, Dabernat S, Morr M, Kumar R, Lacombe ML, Janin J, Lascu I (1999). Catalytic mechanism of nucleoside diphosphate kinase investigated using nucleotide analogues, viscosity effects, and x-ray crystallography. Biochemistry 38, 7265–7272.

Goshima G, Mayer M, Zhang N, Stuurman N, Vale RD (2008). Augmin: a protein complex required for centrosome-independent microtubule generation within the spindle. J Cell Biol 181, 421–429.

Haren L, Remy MH, Bazin I, Callebaut I, Wright M, Merdes A (2006). NEDD1-dependent recruitment of the γ-tubulin ring complex to the centrosome is necessary for centriole duplication and spindle assembly. J Cell Biol 172, 505–515.

Hendrickson TW, Yao J, Bhadury S, Corbett AH, Joshi HC (2001). Conditional mutations in γ-tubulin reveal its involvement in chromosome segregation and cytokinesis. Mol Biol Cell 12, 2469–2481.

Hutchins JR *et al.* (2010). Systematic analysis of human protein complexes identifies chromosome segregation proteins. Science 328, 593–599.

Izumi N, Fumoto K, Izumi S, Kikuchi A (2008). GSK-3β regulates proper mitotic spindle formation in cooperation with a component of the γ-tubulin ring complex, GCP5. J Biol Chem 283, 12981–12991.

Jung MK, Prigozhina N, Oakley CE, Nogales E, Oakley BR (2001). Alanine-scanning mutagenesis of *Aspergillus* γ-tubulin yields diverse and novel phenotypes. Mol Biol Cell 12, 2119–2136.

Keating TJ, Borisy GG (2000). Immunostructural evidence for the template mechanism of microtubule nucleation. Nat Cell Biol 2, 352–357.
Kee JM, Muir TW (2012). Chasing phosphohistidine, an elusive sibling in the phosphoamino acid family. ACS Chem Biol 7, 44–51.
Kollman JM, Polka JK, Zelter A, Davis TN, Agard DA (2010). Microtubule nucleating γ-TuSC assembles structures with 13-fold microtubule-like symmetry. Nature 466, 879–882.
Lacombe ML, Milon L, Munier A, Mehus JG, Lambeth DO (2000). The human Nm23/nucleoside diphosphate kinases. J Bioenerg Biomembr 32, 247–258.
Lai CK, Gupta N, Wen X, Rangell L, Chih B, Peterson AS, Bazan JF, Li L, Scales SJ (2011). Functional characterization of putative cilia genes by high-content analysis. Mol Biol Cell 22, 1104–1119.
Lawo S, Hasegan M, Gupta GD, Pelletier L (2012). Subdiffraction imaging of centrosomes reveals higher-order organizational features of pericentriolar material. Nat Cell Biol 14, 1148–1158.
Lin TC, Gombos L, Neuner A, Sebastian D, Olsen JV, Hrle A, Benda C, Schiebel E (2011). Phosphorylation of the yeast γ-tubulin Tub4 regulates microtubule function. PLoS One 6, e19700.
Luders J, Patel UK, Stearns T (2006). GCP-WD is a γ-tubulin targeting factor required for centrosomal and chromatin-mediated microtubule nucleation. Nat Cell Biol 8, 137–147.
Luders J, Stearns T (2007). Microtubule-organizing centres: a re-evaluation. Nat Rev Mol Cell Biol 8, 161–167.
Mennella V, Keszthelyi B, McDonald KL, Chhun B, Kan F, Rogers GC, Huang B, Agard DA (2012). Subdiffraction-resolution fluorescence microscopy reveals a domain of the centrosome critical for pericentriolar material organization. Nat Cell Biol 14, 1159–1168.
Mikule K, Delaval B, Kaldis P, Jurcyzk A, Hergert P, Doxsey S (2007). Loss of centrosome integrity induces p38-p53-p21-dependent G1-S arrest. Nat Cell Biol 9, 160–170.
Mishra RK, Chakraborty P, Arnaoutov A, Fontoura BM, Dasso M (2010). The Nup107-160 complex and γ-TuRC regulate microtubule polymerization at kinetochores. Nat Cell Biol 12, 164–169.
Moritz M, Braunfeld MB, Guenebaut V, Heuser J, Agard DA (2000). Structure of the γ-tubulin ring complex: a template for microtubule nucleation. Nat Cell Biol 2, 365–370.
Moudjou M, Bornens M (1994). Method of centrosome isolation from cultured animal cells. In: Cell Biology: A Laboratory Handbook, ed. JE Celis, London: Academic Press, 595–604.
Oegema K, Wiese C, Martin OC, Milligan RA, Iwamatsu A, Mitchison TJ, Zheng Y (1999). Characterization of two related *Drosophila* γ-tubulin complexes that differ in their ability to nucleate microtubules. J Cell Biol 144, 721–733.
Piehl M, Tulu US, Wadsworth P, Cassimeris L (2004). Centrosome maturation: measurement of microtubule nucleation throughout the cell cycle by using GFP-tagged EB1. Proc Natl Acad Sci USA 101, 1584–1588.
Postel EH (2003). Multiple biochemical activities of NM23/NDP kinase in gene regulation. J Bioenerg Biomembr 35, 31–40.
Postel EH, Ferrone CA (1994). Nucleoside diphosphate kinase enzyme activity of NM23-H2/PuF is not required for its DNA binding and in vitro transcriptional functions. J Biol Chem 269, 8627–8630.
Rice LM, Montabana EA, Agard DA (2008). The lattice as allosteric effector: structural studies of αβ- and γ-tubulin clarify the role of GTP in microtubule assembly. Proc Natl Acad Sci USA 105, 5378–5383.
Sonnen KF, Schermelleh L, Leonhardt H, Nigg EA (2012). 3D-structured illumination microscopy provides novel insight into architecture of human centrosomes. Biol Open 1, 965–976.
Teixido-Travesa N, Villen J, Lacasa C, Bertran MT, Archinti M, Gygi SP, Caelles C, Roig J, Luders J (2010). The γTuRC revisited: a comparative analysis of interphase and mitotic human γTuRC redefines the set of core components and identifies the novel subunit GCP8. Mol Biol Cell 21, 3963–3972.
Verollet C, Colombie N, Daubon T, Bourbon HM, Wright M, Raynaud-Messina B (2006). *Drosophila melanogaster* γ-TuRC is dispensable for targeting γ-tubulin to the centrosome and microtubule nucleation. J Cell Biol 172, 517–528.
Vogel J, Drapkin B, Oomen J, Beach D, Bloom K, Snyder M (2001). Phosphorylation of γ-tubulin regulates microtubule organization in budding yeast. Dev Cell 1, 621–631.
Vogel P, Read R, Hansen GM, Freay LC, Zambrowicz BP, Sands AT (2010). Situs inversus in Dpcd/Poll$^{-/-}$, Nme7$^{-/-}$, and Pkd1l1$^{-/-}$ mice. Vet Pathol 47, 120–131.
Webb PA, Perisic O, Mendola CE, Backer JM, Williams RL (1995). The crystal structure of a human nucleoside diphosphate kinase, NM23-H2. J Mol Biol 251, 574–587.
Wiese C, Zheng Y (2000). A new function for the γ-tubulin ring complex as a microtubule minus-end cap. Nat Cell Biol 2, 358–364.
Wiese C, Zheng Y (2006). Microtubule nucleation: γ-tubulin and beyond. J Cell Sci 119, 4143–4153.
Yoon JH, Singh P, Lee DH, Qiu J, Cai S, O'Connor TR, Chen Y, Shen B, Pfeifer GP (2005). Characterization of the 3′ → 5′ exonuclease activity found in human nucleoside diphosphate kinase 1 (NDK1) and several of its homologues. Biochemistry 44, 15774–15786.
Zhu H, Coppinger JA, Jang CY, Yates JR III, Fang G (2008). FAM29A promotes microtubule amplification via recruitment of the NEDD1-gamma-tubulin complex to the mitotic spindle. J Cell Biol 183, 835–848.